



## Hydrothermal deposition of zirconia coatings on pre-oxidized BWR structural materials

Z.F. Zhou<sup>a</sup>, E. Chalkova<sup>a</sup>, S.N. Lvov<sup>a,b,c,\*</sup>, P.H. Chou<sup>d</sup>

<sup>a</sup>The Energy Institute, The Pennsylvania State University, University Park, PA 16802, USA

<sup>b</sup>Department of Energy and Mineral Engineering, The Pennsylvania State University, University Park, PA 16802, USA

<sup>c</sup>Department of Materials Sciences and Engineering, The Pennsylvania State University, University Park, PA 16802, USA

<sup>d</sup>EPRI, Palo Alto, CA 94304, USA

### ARTICLE INFO

#### Article history:

Received 13 August 2007

Accepted 10 March 2008

### ABSTRACT

An in situ hydrothermal deposition process is being developed to apply a thin coating of zirconia onto the structural materials used in Boiling Water Reactors as a potential method for mitigating intergranular stress corrosion cracking. The process has successfully deposited ZrO<sub>2</sub> onto as-received interior surfaces of 304 stainless steel and Alloy 600 tubes [Z.F. Zhou, E. Chalkova, S.N. Lvov, P. Chou, R. Pathania, Corros. Sci. 49 (2007) 830]. This paper discusses the application of the coating on specimens with different surface conditions: as-received; ground to remove the as-received surface; and ground and pre-oxidized. For comparable deposition parameters and for a given substrate, the different surface conditions did not influence the morphology or the thickness of the coating, but had a substantial impact on adhesion. As in our previous study, electrochemical potentials of the coated specimens in simulated BWR environment were not clearly lower than those of uncoated specimens [Zhou et al., 2007].

© 2008 Published by Elsevier B.V.

### 1. Introduction

Intergranular stress corrosion cracking (IGSCC) in nuclear reactors remains a significant concern whose occurrence and consequences have to be managed. Since its initial identification in the 1970s, IGSCC has been observed in a range of structural components in vessel internals and in primary piping of boiling water reactors (BWRs) fabricated from 304 and 316 stainless steels, and also from the more resistant 304 L and 316 L versions. The occurrence of IGSCC is associated with high levels of oxidants (O<sub>2</sub> + H<sub>2</sub>O<sub>2</sub>) produced by the radiolysis of water in the BWR core. Several technologies have been developed to mitigate IGSCC in BWRs, among them hydrogen water chemistry (HWC), in which hydrogen is added to the feedwater to reduce the concentration of oxidizing species. But none is a panacea.

HWC, for instance, has some drawbacks. The required amount of hydrogen is expensive. The reducing environment created by the addition of H<sub>2</sub> shifts the equilibrium of the radioactive N<sup>16</sup> species toward the production of volatile, rather than soluble species, resulting in significantly higher radiation fields in the steam circuit. The deposition of radioactive Co<sup>60</sup> onto the interior surfaces of the vessel and of tubing increases, leading to higher shut-down

doses that complicate the management of radiation exposure to plant personnel [2].

In the mid-1990s, General Electric developed Noble Metal Chemical Addition (NMCA), and the process has been widely implemented. Noble metal particles, such as Pt, Pd, and Rh, are deposited onto the surface to catalyze the recombination of oxidants with hydrogen in the vicinity of the surface to form water [3]. The catalysis is rapid, and only a stoichiometric concentration of dissolved H<sub>2</sub>, significantly lower than the amount required for HWC, is necessary to achieve mitigation [4,5]. Since only the environment in the vicinity of the surface is rendered reducing, and the bulk of the water remains oxidizing, the radiation fields in the steam circuit do not rise.

Although noble metals are expensive, the cost of NMCA is not the main driver for the development of alternate mitigation methods. Rather, it is the inability of hydrogen-based techniques to mitigate IGSCC at locations in the BWR (e.g. in the vicinity of the core spray and top guide), where water begins to boil; H<sub>2</sub> partitions preferentially into the steam, and a sufficient amount cannot be maintained in solution [3].

A different approach was proposed to mitigate IGSCC using an inhibitive protective coating (IPC) in mid-1990s [6,7]. The concept of the new approach is based upon the belief that the application of a dielectric coating inhibits the redox reactions on the surface and, therefore, the dissolution of metal at the crack-tip to which they are coupled – without the addition of hydrogen [6–9]. Some promising results have been obtained in laboratories with zirconia

\* Corresponding author. Address: The Energy Institute, The Pennsylvania State University, University Park, PA 16802, USA. Tel.: +1 814 863 8377.

E-mail address: [lvov@psu.edu](mailto:lvov@psu.edu) (S.N. Lvov).

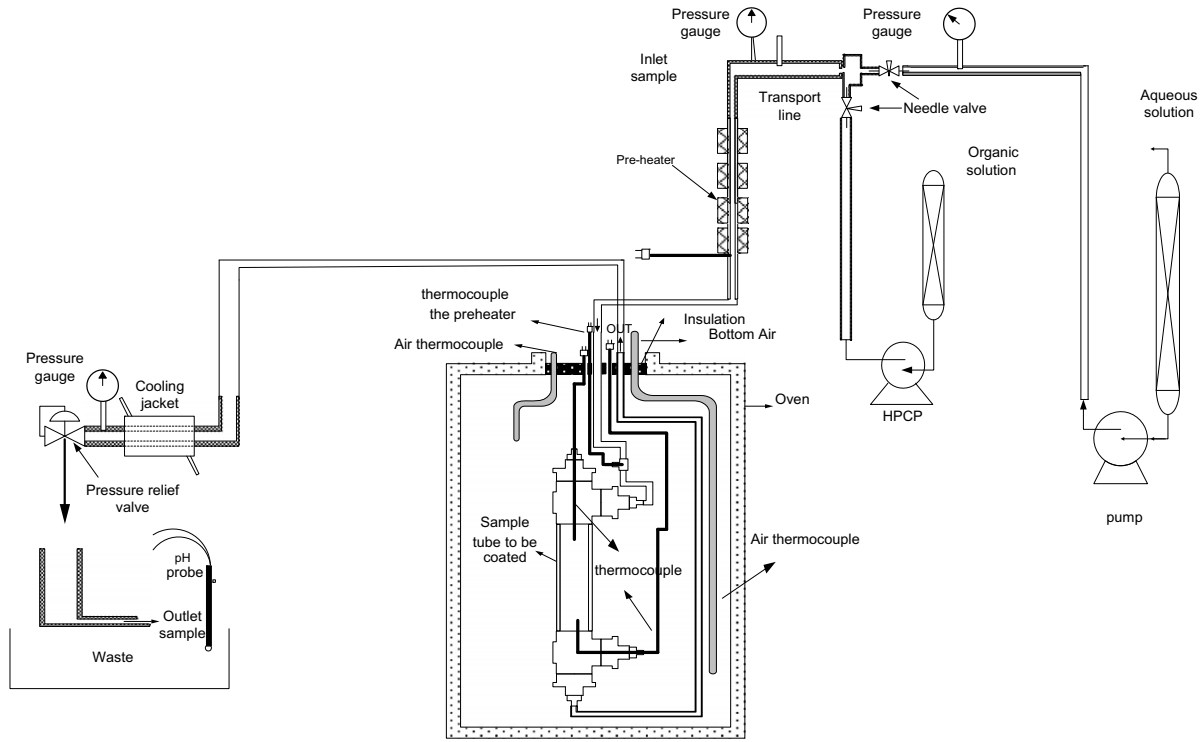


Fig. 1. Schematic of the tubular coating system.

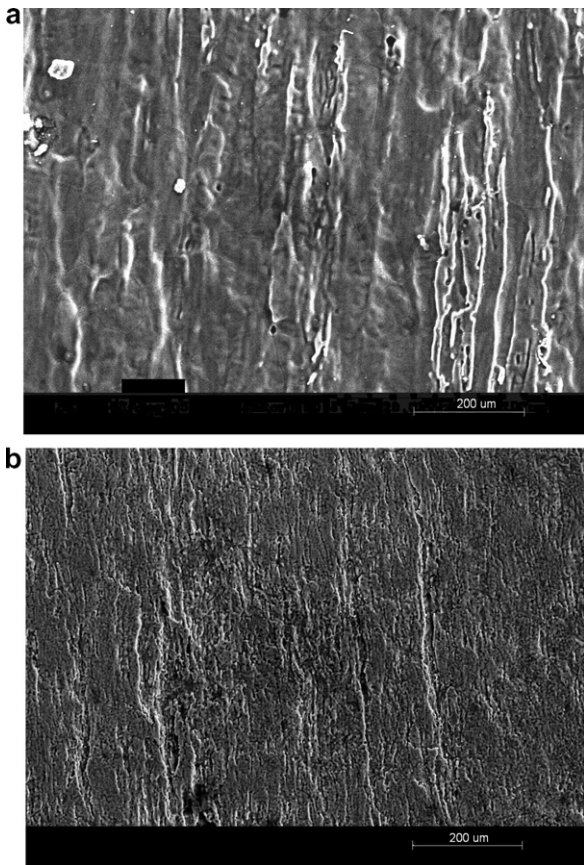


Fig. 2. Surface of as-received specimens: (a) 304 SS; (b) Alloy 600.

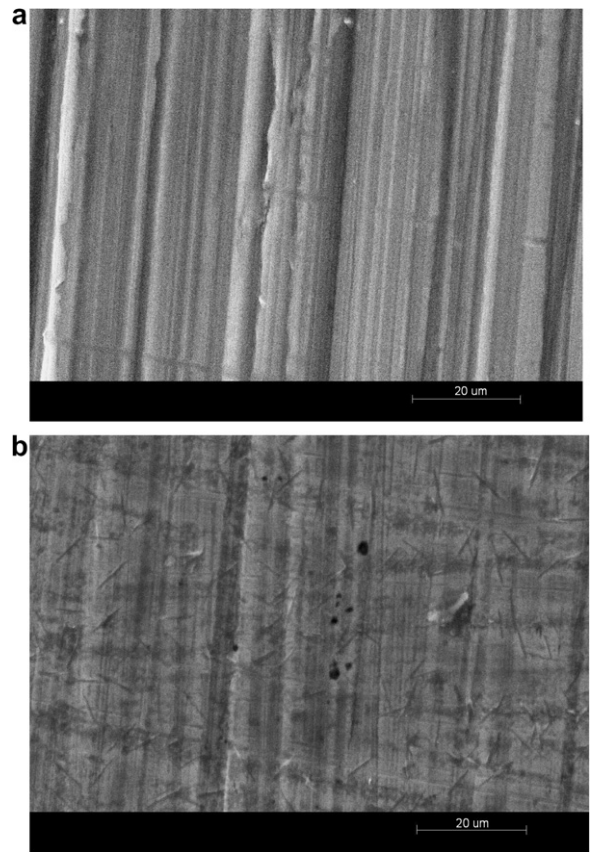


Fig. 3. Surface of ground and polished specimens: (a) 304 SS, (b) Alloy 600.

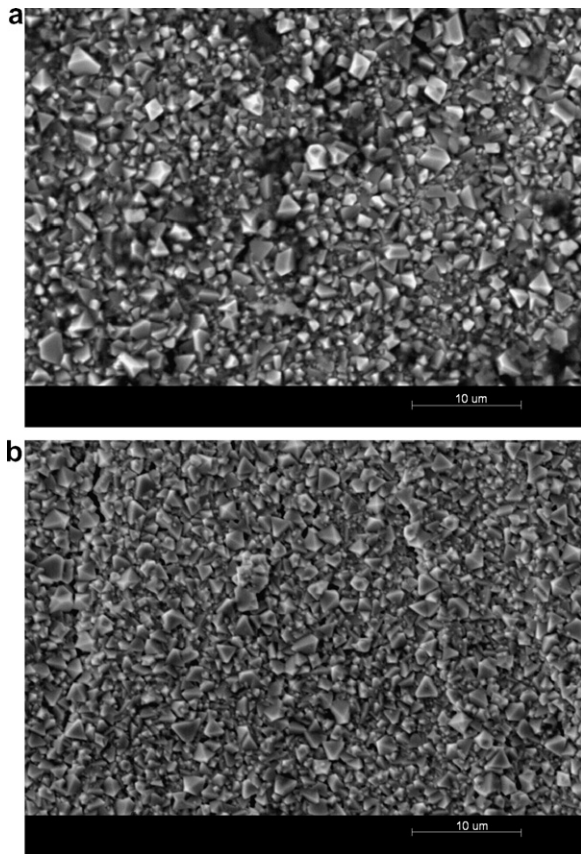


Fig. 4. Surface of pre-oxidized specimens: (a) 304 SS, (b) Alloy 600.

**Table 1**  
Components of the Precursor Solutions

Aqueous precursor solution	Organic precursor solution
ZrO(NO <sub>3</sub> ) <sub>2</sub> ; previously used ZrO(ClO <sub>4</sub> ) <sub>2</sub>	Zr- <i>n</i> -propoxide
Ethylenediaminetetraacetic Acid (EDTA)	1-propanol
Sodium dodecyl sulfate (SDS)	
NaOH	
H <sub>2</sub> O	

or yttria stabilized zirconia (YSZ) coatings prepared by various methods.

Kim and Andresen deposited relatively thick YSZ coatings (75–250 µm) onto stainless steel using plasma spray and demonstrated that the ECP of the coated stainless steel was displaced to as low as –520 mV SHE at 200 ppb O<sub>2</sub> [7,10,11]. Zhou and Macdonald electrochemically deposited fairly thick zirconia coatings (150 µm) onto sensitized stainless steel and showed that the ECP of a coated specimen was 400 mV more negative relative to an uncoated specimen in an air-saturated 0.0005 molar Na<sub>2</sub>SO<sub>4</sub> solution. The crack growth rate of the coated specimen demonstrated a significant reduction compared to uncoated steel [12].

ZrO<sub>2</sub> coatings deposited by other researchers and/or by using other processes, did not always lower the ECP. When Kim and Andresen used a simple dipping process to prepare zirconia coatings on pre-oxidized stainless steel, confirming the presence of Zr by Auger depth profile, the ECP of the treated specimens were only marginally lower [7,10]. Stellwag and Kilian used both sol–gel dipping and hydrothermal deposition to apply zirconia coatings onto stainless steel substrates, in both the as-received and pre-oxidized conditions [13]. The hydrothermally produced coatings, about 0.3 µm

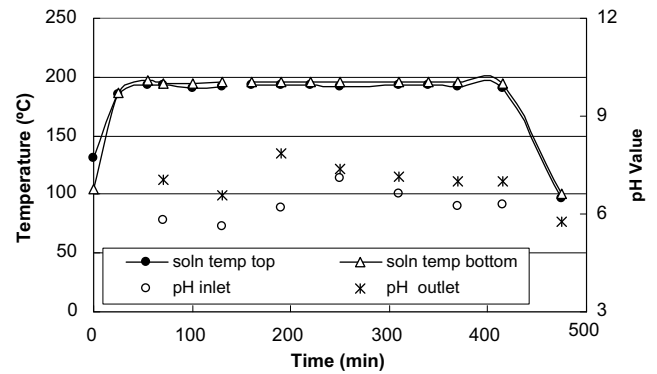


Fig. 5. Temperature and pH during a coating deposition onto 304 SS.

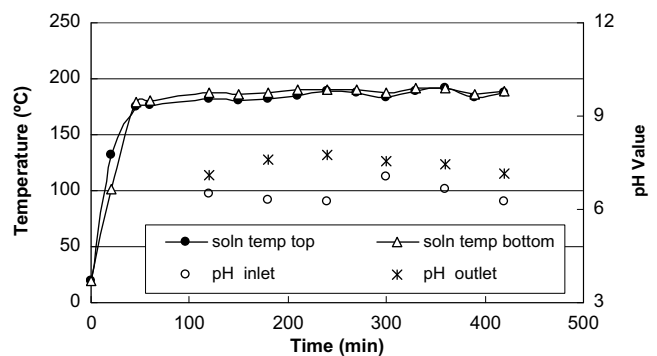


Fig. 6. Temperature and pH during a coating deposition onto Alloy 600.

in thickness, reduced the exchange current density, but increased, marginally, rather than decreased, the ECP. A reduced number of stress corrosion cracks was observed on coated U-bend specimens. Yeh and co-authors also hydrothermally deposited zirconia (and titania) onto pre-oxidized stainless steel [14–15]. They verified by EDS that Zr was present across the surface, but did not report thickness. Their coatings, too, reduced the exchange current density, but had no distinct impact on the ECP. They further investigated, by what are effectively slow strain-rate tests, the effect of the coatings on IGSCC and concluded that the coatings could reduce IGSCC, although they may have been incomplete and discontinuous. Zhou et al. developed a hydrothermal process for the in situ deposition of zirconia and demonstrated that the interior of stainless steel and Alloy 600 tube specimens could be uniformly coated [1,16]. Their coatings did not significantly influence the ECP [1].

This paper describes recent results of zirconia coatings deposited hydrothermally [1,16] onto pre-oxidized 304 stainless steel (304 SS) and Alloy 600 surfaces and of their effect on ECP.

## 2. Experimental system

The hydrothermal process has been used to apply zirconia coatings, in situ, onto the interior surface of tubes and onto exterior surfaces of square and rod specimens. Fig. 1 illustrates schematically the system used to deposit coatings onto the interior surface of tube specimens that are used for the work described in this paper. The reactor is a tube specimen, held at a target temperature, on whose interior wall the zirconia coating will be deposited. The two precursor solutions are stored in separate reservoirs – an organic solution of a Zr-organometallic compound and an aqueous solution consisting of a chelating agent, an oxidant, and a surfactant. The coating

system is filled with pressurized distilled water and heated to the target temperature before reactants are introduced. Initially injected with high-pressure pumps into separate transport tubings, the organic and aqueous solutions meet in a mixing region where the Zr-organometallic reacts with water to form particles of  $\text{Zr}(\text{OH})_4$  that will be deposited as the coating and, in the process, will be transformed into  $\text{ZrO}_2$ . The duration of a typical deposition is 6–10 h.

The  $\text{ZrO}_2$  coatings were examined by scanning electron microscopy (SEM; Hitachi S-3500 N) and Cu  $K\alpha$  X-ray diffraction (XRD; Scintag X2). The coating's adhesion to the substrate was assessed by the tape test described in ASTM Standard D 3359-02 (Test Method B for thin coatings). Permacel 99 tape was used, as recommended by the Standard.

The tube specimens (substrates) were used in one of three surface conditions: (i) as-received; (ii) ground and polished to remove the as-received surface layer, or (iii) oxidized in simulated BWR environment after polishing to produce a representative oxide surface. The term "pre-oxidized" will be used to refer to condition (iii). The outer diameter (OD) and inner diameter (ID) of the 304 SS tubes were 1 in. and 7/8 in., respectively. The dimensions of the Alloy 600 tubes were 7/8 in. OD and 13/16 in. ID.

A  $\text{ZrO}_2$ -coated tube specimen and an uncoated pre-oxidized stainless steel tube were placed in the same autoclave; measurements were obtained simultaneously from both, using an externally pressure-balanced Ag/AgCl reference electrode filled with  $0.1 \text{ mol kg}^{-1}$  KCl.

### 3. Results

#### 3.1. Surface preparation

The deposition of  $\text{ZrO}_2$  coatings onto as-received surfaces of tube specimens were reported in greater detail elsewhere [1,16]. This paper compares the deposition onto three different surface conditions: (i) as-received; (ii) mechanically ground and polished and (iii) pre-oxidized. Fig. 2 illustrates the typical appearances of the as-received interior surfaces of 304 SS and Alloy 600 tubes (Condition i). They are microscopically rough. The as-received surface condition (e.g. surface composition) depends on details of thermomechanical processing and of chemical surface treatment and differs across different products and different manufacturers. Of particular concern are possible (and ill-defined) residue/contaminants on the surface. The tubes were ground to remove several microns of material (and prior surface history), polished to average roughness number ( $R_a$ ) 16–32, and degreased with acetone, to establish reproducibility (Condition ii). The ground and polished surface of 304 SS appears somewhat rougher than that of Alloy 600 (Fig. 3). Twins are frequently observed on the surface of the latter.

Because deposition onto a surface is likely to be sensitive to the character of that surface, it is important to ascertain the ability to deposit the coating, and the quality of that coating, on oxidized surfaces representative of those that develop in the BWR NWC environment. Therefore some, mechanically ground and polished tube specimens were installed in a flow loop, and their interior surfaces were pre-oxidized by flowing  $288^\circ\text{C}$  low-conductivity water ( $\leq 0.3 \mu\text{S/cm}$  at the outlet) containing 250 ppb  $\text{O}_2$  and 10 ppb  $\text{Zn}^{2+}$  for 500 h (Condition iii). Surface Condition (ii), rather than the as-received surface, was the starting point of preoxidation, because a previous study had indicated that variability in the as-received surface condition had resulted in inconsistent oxide morphology [18]. Fig. 4 shows the pre-oxidized interior surfaces of 304 SS and Alloy 600 tube specimens, covered uniformly by fine oxide particles; the surfaces developed the expected morphologies [18]. It has been suggested by Macdonald that the visible oxide particles are  $\text{Fe}_3\text{O}_4$  on stainless steel [19] and by Mintz and Devine that they are

$\text{Ni}_3\text{O}_4$  (which are often loose and non-adherent) on Alloy 600 [20]. Since the total oxide thicknesses were less than  $1 \mu\text{m}$ , reflections originating from the oxides in the X-ray spectra obtained by this study are expected to be weak. A low-intensity reflection at  $\sim 36^\circ$  was observed from some substrates of 304 SS and Alloy 600 and may be the (3 1 1) reflection of both  $\text{Fe}_3\text{O}_4$  and  $\text{Fe}_2\text{O}_3$  on the former (Fig. 9), and may be the (1 1 1) reflection of NiO on the latter (Fig. 12). For Alloy 600, the assignment does not appear consonant with that of Mintz and Devine.

#### 3.2. Coating process and conditions

The coating-formation process has been described in detail elsewhere [1,16]. Table 1 gives the components of the aqueous and organic precursor solutions. Figs. 5 and 6 plot process pH and temperature, with respect to time, during typical depositions

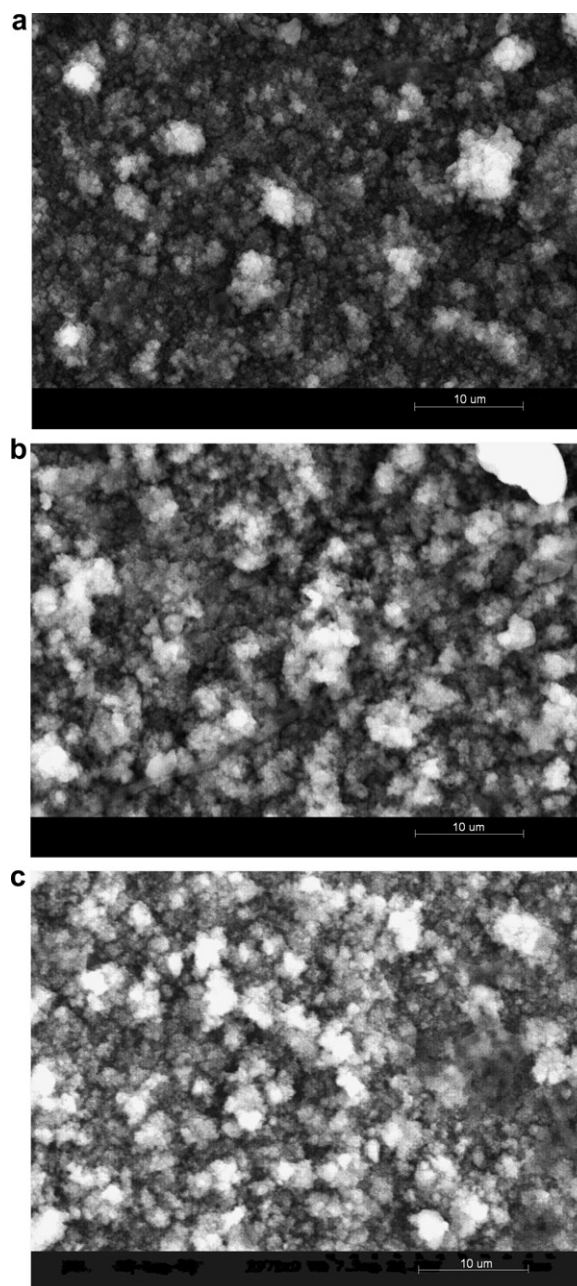


Fig. 7. Coated surfaces of 304 SS specimens: (a) as-received, (b) ground and polished, and (c) pre-oxidized.

onto 304 SS and Alloy 600, respectively. The temperature variation over the length of the specimen(s) is small. The pH was in the range of 6–8, with the value at the outlet slightly higher than at the inlet. To compare the effect of different surface conditions on deposition, two tube segments of different surface conditions were joined with a Swagelok union and coated simultaneously.

### 3.3. Microstructures of coatings

Fig. 7 exhibits SEM images of coatings deposited on as-received, ground and polished, and pre-oxidized surfaces of 304 SS specimens. The latter two were coated simultaneously, and the process

temperature and pH are shown in Fig. 5; while the first was coated separately under the same nominal conditions. The three coatings appear similar; all were composed of finely agglomerated particles approximately 100 nm in diameter.

The X-ray diffraction patterns indicate that the tetragonal phase of  $ZrO_2$  was deposited, as shown in Figs. 8 and 9. The average thickness of the  $ZrO_2$  coating on the pre-oxidized 304 SS specimen was  $1.0\ \mu\text{m}$  according to metallographic cross-section and  $0.58\ \mu\text{m}$  according to Rutherford Backscattering Spectrometry (RBS). RBS measured area atom density ( $Zr\ \text{atoms}/\text{cm}^2$ ) that was recalculated to obtain thickness using  $6.1\ \text{g}\ \text{cm}^{-3}$  as the density of  $ZrO_2$  (fully dense); if the film were less than fully dense because of porosity, the calculated thickness would be greater.

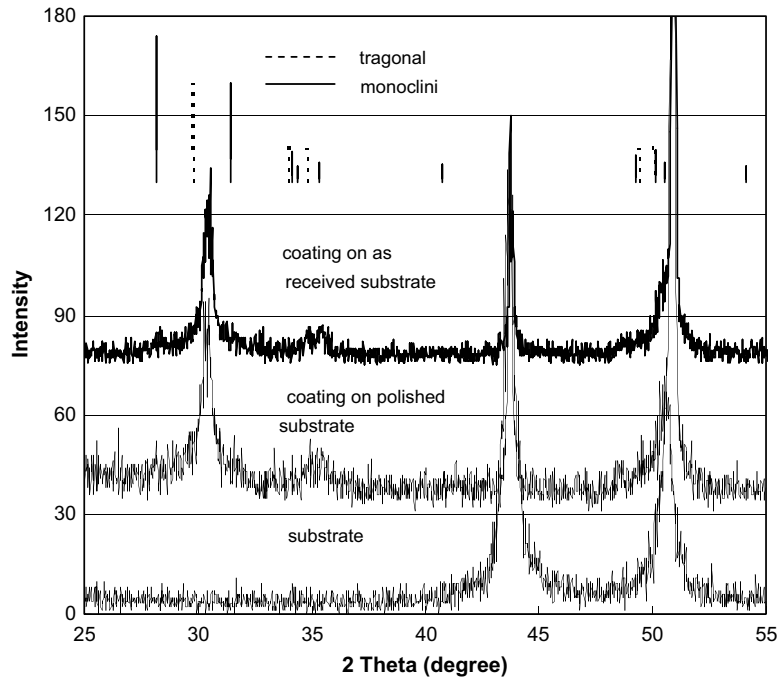


Fig. 8. X-ray spectra of  $ZrO_2$  coatings deposited on as-received, and ground and polished 304 SS specimens.

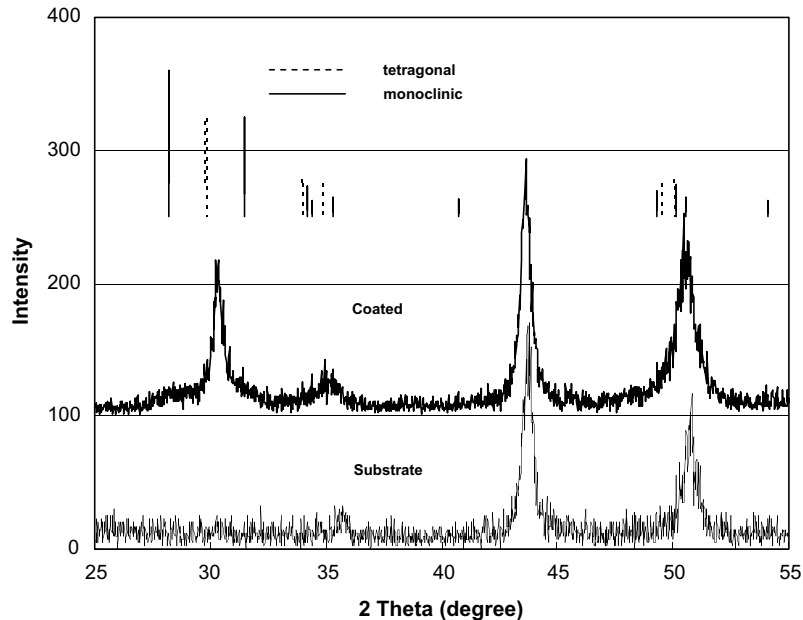


Fig. 9. X-ray spectrum of a  $ZrO_2$  coating deposited on a pre-oxidized 304 SS specimen.

Fig. 10 displays SEM images of coatings deposited on as-received, ground and polished, and pre-oxidized surfaces of Alloy 600 specimens. Again, the latter two were coated simultaneously, and the process temperature and pH are shown in Fig. 8, while the first was coated separately under the same nominal conditions. The three coatings appear similar, consisting of agglomerated particles approximately 500 nm in diameter; comparison of Figs. 10 and 8 reveals that the degree of agglomeration is greater than that observed in coatings on 304 SS.

A mixture of monoclinic and tetragonal  $ZrO_2$  phases was deposited according to the X-ray spectra of Figs. 11 and 12, whereas, on 304 SS, only tetragonal  $ZrO_2$  was evident. This may be interpreted as the influence of the different native surface oxides on 304 SS and Alloy 600.

The ability to lay down a coating on three different surface conditions of 304 SS and Alloy 600, each, implies that the process of deposition is tolerant. If the deposition process is based on the electrostatic attraction of opposite surface charges, on the surface and on the particles, as has been proposed, [1,16] then the zeta potential of the native oxides associated with the different surface conditions are similar enough to allow deposition. The adhesion of the coating to the substrate, however, is not as tolerant to surface conditions.

### 3.4. Coatings adhesion

Fig. 13 summarizes the results of tape adhesion tests performed on a large number of coatings. Coatings deposited on as-received and pre-oxidized surfaces demonstrated very good and consistent adhesion, while those deposited on ground and polished surfaces gave values for rip-off that varied from 0% to 95%, for both 304 SS and Alloy 600. While data for Alloy 600 is limited, it is consistent with the trend demonstrated more clearly by 304 SS. Because the coatings deposited on specimens of all three surface conditions appear similar, as noted in the previous section, the adequacy of a coating's adhesion cannot be assessed by its appearance.

The authors speculate on three possible reasons for the poor adhesion of coatings deposited on ground and polished surfaces, two centered around the character of the oxide. First, a ground and polished surface may not mechanically "anchor" the coatings as effectively. A smoother surface may provide fewer "anchoring" sites that interlock with the coating. In addition, the grinding and polishing process may have left (relatively) loosely embedded (metal and/or oxide) particles in the surface, since no subsequent chemical surface treatment was applied. The apparent adhesion of a coating that is deposited on top of these particles would be limited by the adhesion of these defects to the surface. Second, the environment during and following grinding and polishing may not allow the native oxide to establish as completely, with the same adhesion, thickness and/or quality, as the as-received or pre-oxidized surfaces. An appropriate concentration of oxidant in the precursor solution modifies the oxide surface to enhance bonding between the coating and the substrate [1,16]; concentrations either too low or too high can lead to poor adhesion. The amount used in this study may be effective for the oxides on as-received and pre-oxidized surfaces, but may be ineffective for thinner oxide present on ground and polished surfaces. Third, the zeta potential of the ground and polished surface may be sufficiently different from the as-received and the pre-oxidized surfaces to decrease the strength of electrostatic interaction and reduce resultant adhesion.

The adhesion of coatings deposited on both pre-oxidized 304 SS and Alloy 600 were very good. This is an important observation, since the goal is to deposit a thin coating of  $ZrO_2$  onto the oxidized surfaces of existing BWR structural materials to mitigate IGSCC.

### 3.5. ECP measurement

Fig. 14 plots the ECP values of a (uncoated) pre-oxidized 304 SS specimen and a  $ZrO_2$ -coated pre-oxidized 304 SS specimen with respect to dissolved  $O_2$  concentration (0.45–1 ppm) in deionized water at 265 °C. Since the measured ECP values of pre-oxidized stainless steel reported by different laboratories span a wide range [21], attributed to differences in flow rate (relative to surface area capable of consuming oxygen) and to differences in sampling dissolved  $O_2$  (e.g. whether at the inlet or the outlet), among other factors, the absolute values of the ECP are less significant than the relative values between the two specimens.

And their ECPs are not significantly different. While not presented in this Figure, the uncoated specimen, in fact, had slightly lower ECP than the coated specimen at some oxygen concentrations.

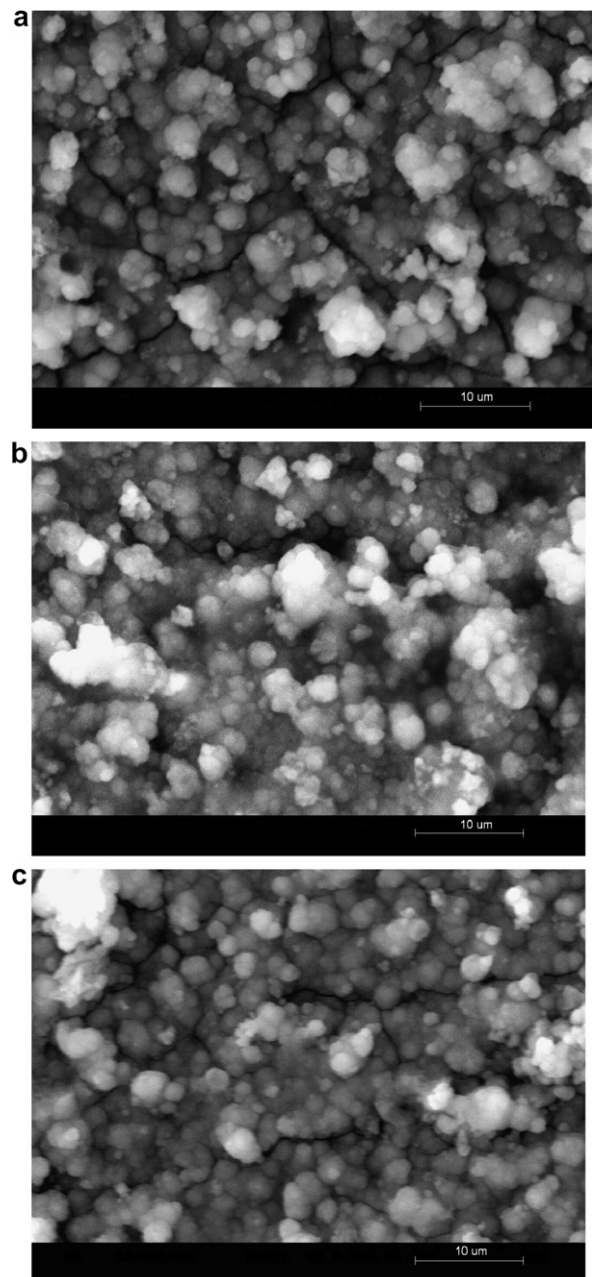


Fig. 10. Coated surfaces of Alloy 600 specimens: (a) as-received, (b) ground and polished, (c) pre-oxidized.

**4. Discussion**

The studies that have been conducted in different laboratories suggest that inhibitive protective coatings (IPCs) can reduce the exchange current density, crack initiation, and growth; however, the data is neither uniform (with different groups performing different tests and/or using different conditions) nor entirely consistent. It has been established that in the BWR environment, the propaga-

tion of SCC cracks in stainless steel is dramatically reduced when the ECP is less than  $-230$  mV SHE [17]. There exist uncertainties as to whether IPCs will give rise to more negative ECPs relative to an uncoated surface [14–15]. Indeed, Yeh et al. suggest that an IPC need not induce a more negative ECP in order to be effective against IGSCC.

If the coating were perfect, there is little doubt that IGSCC will be prevented; after all, the metal is separated from the corrosive

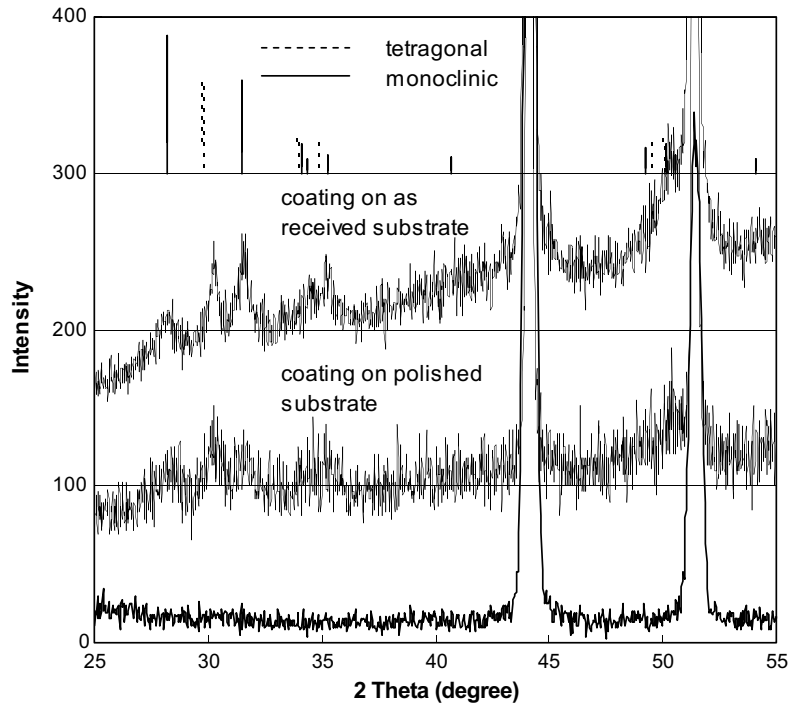


Fig. 11. X-ray spectra of  $ZrO_2$  coatings deposited on as-received, and ground and polished Alloy 600 specimens.

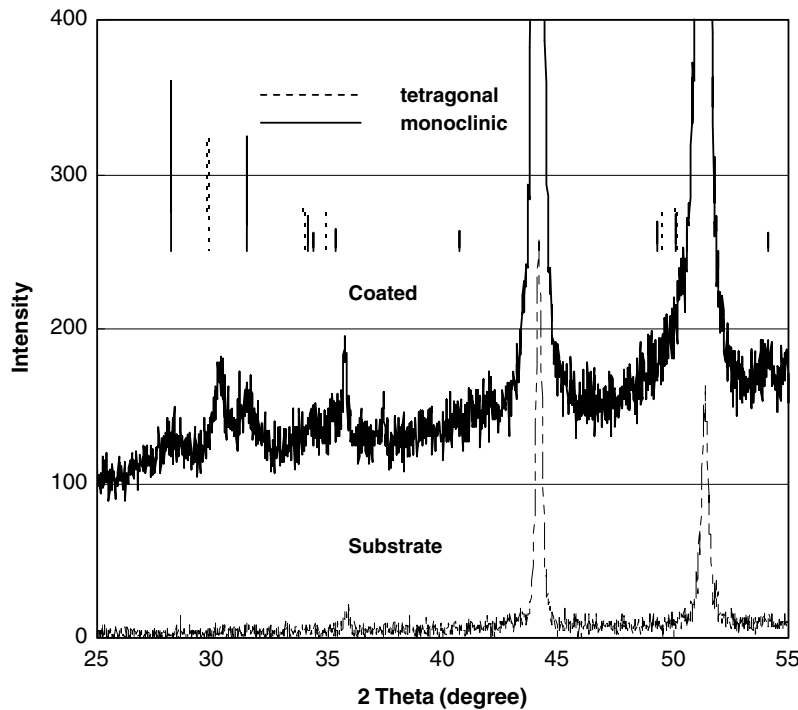


Fig. 12. X-ray spectrum of a  $ZrO_2$  coating deposited on a pre-oxidized Alloy 600 specimen.

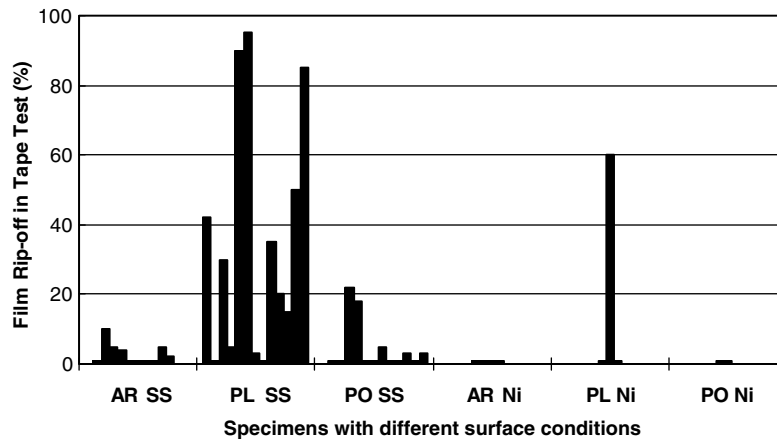


Fig. 13. Summary of the results of tape adhesion tests performed on 304 SS and Alloy 600, each with different surface conditions. AR SS: as-received 304SS; PL SS: ground and polished stainless steel; PO SS: pre-oxidized 304 SSI; AR Ni: as-received Alloy 600; PL Ni: ground and polished Alloy 600; PO Ni: pre-oxidized Alloy 600.

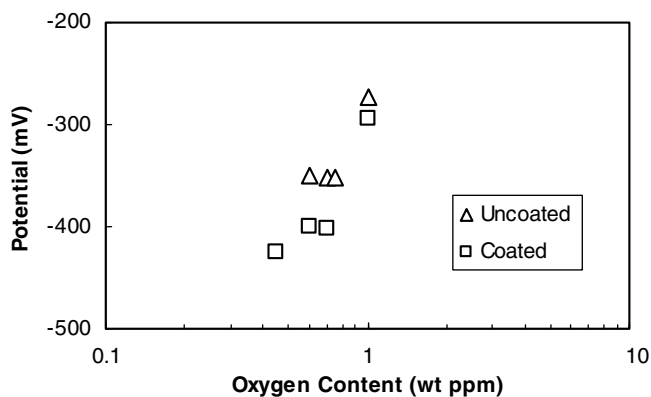


Fig. 14. ECP values of a (uncoated) pre-oxidized 304 SS specimen and a  $ZrO_2$ -coated pre-oxidized 304 SS specimen with respect to dissolved  $O_2$  concentration in deionized water at 265 °C.

environment. However, disagreement arises upon consideration of a crack in the coating (a “coating-crack”).

Yeh et al. (and also MacDonal) believe that there is extensive coupling between an IGSCC crack tip (and in this case, the metal at the bottom of a coating-crack) and the external surfaces. Therefore, Yeh uses a mixed-potential model that includes redox reactions on the external surface (and that assumes the IPC coating is not perfectly insulating) for interpretation. If the presence of the coating decreases the (absolute) rate of reduction occurring on the external surface, then the rate of dissolution of metal at the crack tip, to which it is coupled, also decreases. However, the ECP is determined by the relative decreases in the rates, on the external surface, of reduction (e.g. that of  $O_2$ ) versus oxidation (e.g. that of general corrosion of the coated metal substrate, with species diffusing through the coating). If the rate of reduction reaction is depressed significantly relative to the rate of oxidation, then the ECP will shift lower; if the rate of oxidation is depressed significantly relative to the reduction reaction, then the ECP will shift higher. Consequently, Yeh argues, it is possible for the coating to mitigate IGSCC without inducing a more negative ECP.

Kim and Andresen have an alternate viewpoint. If the coating develops a crack, as long as the coating-crack is sufficiently restrictive and long, it will form an artificial stagnant layer of solution through which oxidants must diffuse; the oxidant flux that reaches the metal will be insufficient to shift the ECP to deleteriously high values; and certainly not as high as, say,  $-230$  mV [10]. On the other hand, if the coating-crack is severe, and the oxidant flux that reaches the metal raises the ECP above  $-230$  mV, then mitigation

is lost. In their interpretation, ECP is a clear indication of whether the coating mitigates IGSCC.

The two descriptions differ in a potentially important and practical way. That of Yeh is, in principle, more tolerant of damage – as long as sufficient area is covered by the coating so that the absolute rate of reduction on the external surface is sufficiently decreased, IGSCC will be mitigated. The description of Kim and Andresen suggest that the primary benefit of the coating is the prevention of crack initiation of the area covered by the coating, for it seems difficult to insure that cracks which develop during the processing/deposition of the coating or during subsequent service will always remain sufficiently geometrically restrictive with respect to the oxidant flux that reaches the metal. One should note that the prevention of crack initiation may potentially be a significant benefit, even if there is no benefit with respect to crack propagation.

The ECP measurements from this work agree with previous results reported by the authors, [1,16] as well as with those of Yeh et al. [14], and Stellwag and Killian [13], but not with those of Kim and Andresen [10] and Zhou and Macdonald [12]. Additional studies are necessary to resolve the disagreement, which might be correlated with the very different coating thicknesses produced by the different groups.

The coatings produced in this study ( $1\text{--}2\ \mu\text{m}$ ) were marginally thicker than those of Stellwag and Kilian ( $0.3\ \mu\text{m}$ ), but substantially thinner than those of Kim and Andresen ( $75\text{--}250\ \mu\text{m}$ ) and Zhou and Macdonald ( $150\ \mu\text{m}$ ). Thick coatings, therefore, appear more effective in reducing ECP and may be rationalized by the lower expected probability of severe defects that penetrate greater thicknesses. For example, Figs. 7 and 10 illustrate that the  $ZrO_2$  coatings are comprised of consolidated particles. There is a distribution of particle sizes, and the larger ones are significant relative to the thickness of the coating ( $1\text{--}2\ \mu\text{m}$ ), contributing to unevenness and perhaps to the formation of defects, such as the micro-cracks and possible voids in Fig. 10. If these defects could be eliminated to produce a more uniform coating (e.g. by changing the process conditions to consolidate smaller particles), it may be possible to achieve the lower ECP values observed in thicker coatings.

## 5. Conclusions

This study investigates the in situ hydrothermal deposition of thin ( $1\text{--}2\ \mu\text{m}$ )  $ZrO_2$  coatings on 304 SS and Alloy 600 specimens with different surface conditions: as-received; ground and polished; and pre-oxidized. In particular, it has been ascertained that such coatings can be deposited onto pre-oxidized 304 SS and Alloy 600 surfaces; 304 SS and Alloy 600 are prototypical BWR structural



alloys. The pre-oxidized surfaces, whose character may influence deposition, simulate those that develop in the BWR NWC environment. Adherent coatings were obtained on the as-received and the pre-oxidized surfaces of both 304 SS and Alloy 600; the adhesion of the coatings deposited on the ground and polished surfaces was, in general, worse, for both alloys. For all surface conditions, tetragonal  $ZrO_2$  was the phase deposited on 304 SS, while a mixture of monoclinic and tetragonal phases was deposited on Alloy 600. ECP measurements conducted on a  $ZrO_2$ -coated pre-oxidized 304 SS specimen did not demonstrate significantly more negative ECPs relative to an uncoated pre-oxidized 304 SS specimen.

### Acknowledgements

This work was supported by the Electric Power Research Institute through its BWR Vessels and Internals Program. Dr S.C. Menasian of the Cornell Center for Materials Research at Cornell University is thanked for conducting the RBS analysis of coating thickness. Also, we thank Mr R. Kumar for valuable contributions to this study.

### References

- [1] Z.F. Zhou, E. Chalkova, S.N. Lvov, P. Chou, R. Pathania, *Corros. Sci.* 49 (2007) 830.
- [2] Y.-J. Kim, P.L. Andresen, in: Eleventh International Conference on Environmental Degradation of Materials in Nuclear Systems, Stevenson, WA, 2003, p. 526.
- [3] S. Hettiarachchi, G.P. Wozadlo, P.L. Andresen, T.P. Diaz, R.L. Cowan, in: Proceedings of 7th International Symposium on Environmental Degradation of Materials in Nuclear Power System-Water Reactors, NACE, Houston, TX, 1995, p. 735.
- [4] S. Hettiarachchi, R.J. Law, T.P. Diaz, R.L. Cowan, in: Eighth International Conference on Environmental Degradation of Materials in Nuclear Power System-Water Reactors, August 10–14, 1997, p. 535.
- [5] S. Hettiarachchi, T.P. Diaz, P.L. Andresen, Y.-J. Kim, in: The 3rd International Water Chemistry Conference, San Francisco, 2004, p. 849.
- [6] D.D. Macdonald, T.K. Yeh, A.T. Motta, *Corrosion* 95, 1995, Paper No. 403.
- [7] Y.-J. Kim, P.L. Andresen, *Corrosion* 96, 1996, Paper No. 105.
- [8] D.D. Macdonald, *Corrosion* 48 (1992) 194.
- [9] D.D. Macdonald, P.-C. Lu, M. Urquidi-Macdonald, T.-K. Yeh, *Corrosion* 52 (1996) 768.
- [10] Y.-J. Kim, P.L. Andresen, *Corrosion* 54 (1998) 1012.
- [11] P.L. Andresen, Y.-J. Kim, US Patent No. 5,465,281.
- [12] X. Zhou, I. Balachov, D.D. Macdonald, *Corros. Sci.* 40 (1998) 1349.
- [13] B. Stellwag, R. Kilian, *Water Chem. Nucl. Reactor Syst.* 32 (2000) 127.
- [14] T.-K. Yeh, M.-Y. Lee, C.-H. Tsai, *J. Nucl. Sci. Technol.* 39 (2002) 531.
- [15] T.-K. Yeh, C.-H. Tsai, C.-H. Chen, C.-M. Cheng, R.-F. Sheng, F. Chu, in: The 3rd International Water Chemistry Conference, San Francisco, 2004, p. 627.
- [16] Z.F. Zhou, S.N. Lvov, S.S. Thakur, X.Y. Zhou, P. Chou, R. Pathania, in: The 3rd International Water Chemistry Conference, San Francisco, 2004, p. 602.
- [17] P.L. Andresen, F.P. Ford, S.M. Murphy, J.M. Perks, in: Fourth International Conference on Environmental Degradation of Materials in Nuclear Power System – Water Reactors, NACE, Houston, TX, 1990, p. 1/83.
- [18] R.J. Law, Private communications.
- [19] D.D. Macdonald, *Pure Appl. Chem.* 71 (1999) 951.
- [20] T.S. Mintz, T.M. Devine, *Key Eng. Mater.* 261–263 (2004) 875.
- [21] D.D. Macdonald, *Corrosion* 48 (1992) 194.